Journal of Hazardous Materials 494 (2025) 138544

Contents lists available at ScienceDirect

Journal of Hazardous Materials

journal homepage: www.elsevier.com/locate/jhazmat

A comprehensive mechanism of polyester enzymatic depolymerization: A novel singular key parameter for streamlined eco-design

Sylvie Dufour [a,b,*], Samira Benali [a], Alice Delacuvellerie [b], Yoann Paint [c], Philippe Dubois [a], Ruddy Wattiez [b], Jean-Marie Raquez [a,*]

[a] Laboratory of Polymeric and Composite Materials, University of Mons, Belgium
[b] Laboratory of Proteomic and Microbiology, University of Mons, Belgium
[c] Materia Nova, Mons, Belgium

HIGHLIGHTS

- Unify the physico-chemical parameters known from the literature by means of a Design of Experimental.
- Non-enzymatic and enzymatic degradations are studied at the same time.
- A flux diagram highlighting all these parameters, with their hirerchization.
- An illustrated mechanism showing, step by step, how the two types of degradation influence each other.
- Plastics degradation understanding through a single key parameter: the soaked material glass transition temperature (T_g^s).

GRAPHICAL ABSTRACT

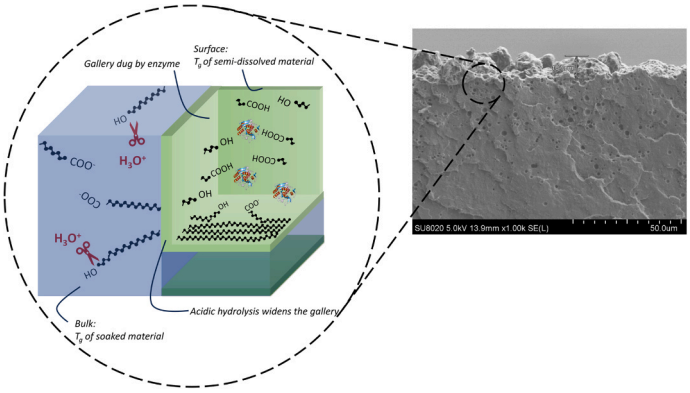

ARTICLE INFO

Keywords:
Enzymatic depolymerization
Mechanism
Polyester
Recycling
Eco-design

ABSTRACT

Plastic pollution persists due to polymers' resistance to depolymerization, making eco-design and enzymatic recycling essential for sustainability. However, understanding plastic depolymerization is complex, and studies often separate enzymatic from non-enzymatic degradation, despite their interconnectedness in practice. This study aims to simplify this process, unifying key factors into a single mechanism using polylactide (PLA) as a model. We demonstrate that the local glass transition temperature of the soaked material (T_g^s) —a novel parameter—is the central factor enabling chain mobility for enzyme interaction, with chain mobility as the primary driver in degradation. Enzymatic hydrolysis initiates perforation, triggering non-enzymatic depolymerization when chain-end density is sufficient. This unified mechanism complements enzymologists' work, providing an innovative pathway to optimize enzymatic plastic recycling and accelerate polyester degradation under practical conditions.

* Corresponding authors at: Laboratory of Polymeric and Composite Materials, University of Mons, Belgium.
E-mail addresses: sylvie.dufour@umons.ac.be (S. Dufour), jean-marie.raquez@umons.ac.be (J.-M. Raquez).

https://doi.org/10.1016/j.jhazmat.2025.138544
Received 12 February 2025; Received in revised form 18 April 2025; Accepted 7 May 2025
Available online 8 May 2025

1. Introduction

The role of plastics in modern society is undeniable. Their versatility, low cost, and superior mechanical properties, particularly lightness, make them indispensable across industries. However, the current plastics model is unsustainable [1,2]. Plastics are at the center of environmental and health concerns, mainly due to (1) their production from fossil resources and (2) improper waste management, leading to accumulation in ecosystems. This depletion of fossil fuels, coupled with persistent microplastic pollution, poses significant challenges [3,4]. While the reliance on petroleum is being addressed by bio-based polymers (*e.g.*, bio-polyethylene terephthalate (Bio-PET), polylactide (PLA), bio-polypropylene (Bio-PP), bio-polybutylene succinate (Bio-PBS)), projected to grow to 9.3 million tons by 2027 [5,6], the primary challenge remains end-of-life management. Plastics' durability, advantageous during use, results in environmental persistence as microplastics, with evident detrimental impacts [7–9].

Consequently, both scientific and political communities promote a circular economy, valuing waste as raw material for new plastics [5,10]. Chemical recycling, particularly enzyme-catalyzed hydrolysis, emerges as a promising method [11, 12]. Carbios has demonstrated industrial feasibility for enzymatic poly(ethylene terephthalate) (PET) recycling [13]. Enzymes enable depolymerization using water as a solvent, at mild temperatures, with high substrate selectivity, avoiding additional sorting. This bio-inspired recycling mimics nature's enzymatic degradation of polymers [14]. Enzymatic depolymerization is also critical in biodegradable plastics, offering potential to prevent microplastic formation if the process is sufficiently rapid [15–17].

In a circular economy context, depolymerization represents the most effective route for plastics. Returning polymers to their monomers could enable a truly sustainable approach. However, optimizing plastics for enzymatic depolymerization requires eco-design, considering end-of-life factors. Numerous parameters influence enzymatic hydrolysis, complicating our understanding of this process and eco-design success (Fig. 1).

The objective of our study is to unify the most relevant parameters in a way to sustain a successful eco-design approach, highlighting unified multi-factor process. As a model polymer, PLA was herein selected to study both enzymatic and non-enzymatic depolymerizations. Indeed, despite the existence of dozens of enzymes capable of degrading PLA, it is resistant to depolymerization, resulting in the formation of microplastics. This clearly shows that scientists lack knowledge of the mechanism that exists between a solid polymer and the enzyme. Moreover, polylactide is the most produced biobased plastic thanks to its superior tensile strength and modulus, with an annual production that is expected to increase from 300,000 to 3000,000 tonnes by 2027 [6]. However, PLA biodegradation is only achievable in industrial composting environments, generating debate on its classification as a "green" material [18]. Another advantage of PLA is its synthesis from two monomers, L-lactide (PLLA) and D-lactide (PDLA), influencing mechanical properties. Typically, as the amount of D-monomers relative to L-monomers increases, PLA is less able to crystallize. Nano-reinforcements are commonly used to tailor PLA's properties for specific applications. As a polyester, PLA undergoes hydrolysis via ester bond cleavage, forming alcohol and carboxylic acid, which accelerates hydrolysis through acid autocatalysis [19, 20]. The process, extensively studied, follows an exocision mechanism where end-chain esters (α-esters) hydrolyze faster than internal chain esters (β-esters) [19]. Factors such as water absorption, oligomer diffusion, and solubility—determined by PLA's molar mass and crystallinity—govern hydrolysis, leading to surface or bulk degradation [20, 21]. In contrast, enzymatic hydrolysis of PLA has received less attention [22, 23]. While dozens of enzymes, primarily hydrolases (*e.g.*, esterases, cutinases, lipases), can degrade PLA, it is considered non-biodegradable under natural conditions [15]. Enzymatic hydrolysis is faster in amorphous regions than crystalline ones [24], but only surface crystals can degrade by enzyme [25–27]. Proteinase K has been reported as a highly effective enzyme for PLA degradation, preferentially cleaving β-ester bonds along the polymer chain, highlighting its endoenzyme nature [28, 29]. Key studies from the 2000s further demonstrated that enzyme adsorption, surface hydrophilicity, and nanomechanical reinforcement affect degradation rates [30–32].

Another challenge that hinders the success of eco-design is that the scientific literature on

polyester hydrolysis is still divided into enzymatic and non-enzymatic studies. To the best of our knowledge, these two types of degradation have never been examined simultaneously. However, existing literature demonstrates that the morphological and chemical changes in the material vary significantly during hydrolytic

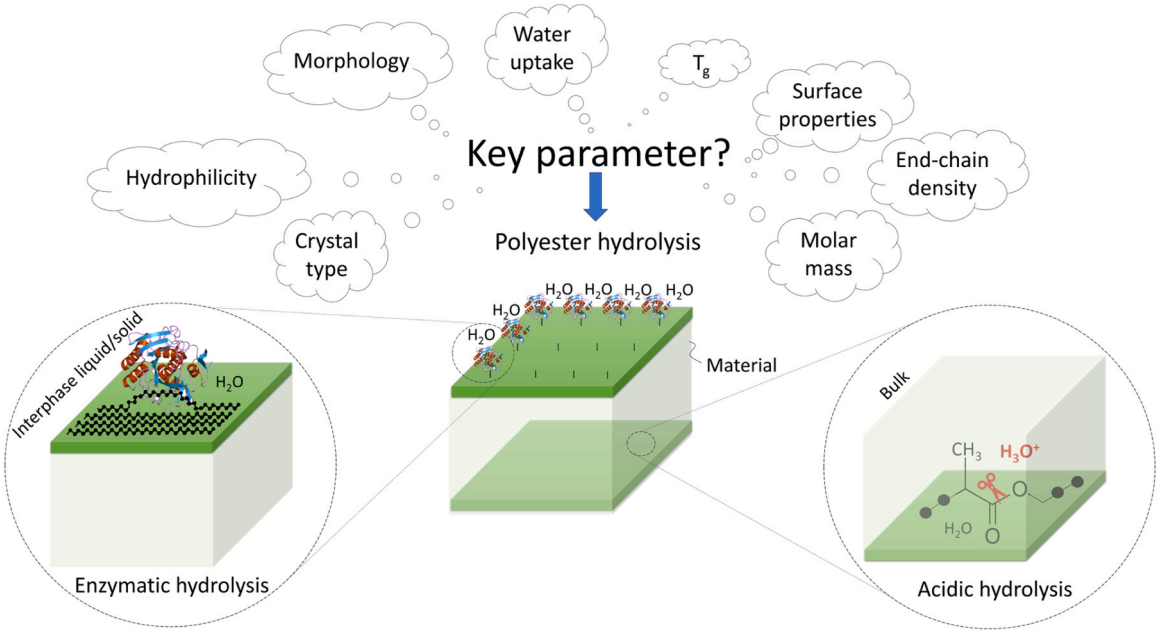

Fig. 1. Main parameters involved in polyester hydrolysis. Hydrolysis can be enzymatic (interphase liquid/solid) or acidic (bulk), and both types of catalysis can occur simultaneously.

degradation, regardless of whether it is enzyme-, base-, or acid-catalyzed. These changes during material breakdown could potentially allow for other types of catalysis to occur, a possibility that has never been considered before.

Upon the type of degradation, there are several behaviors reported: (a) due to the enzyme large size, it cannot penetrate between the bulk PLA chains, meaning the PLA-enzyme interaction occurs predominantly at the water/material interface [30]; (b) non-enzymatic surface hydrolysis is negligible compared to surface enzymatic hydrolysis. Furthermore, Michel Vert's work in the 1990s demonstrated that samples thinner than 0.5 mm preferentially degraded in bulk [33]; (c) non-enzymatic bulk hydrolysis can only be acidic. While a few hydroxyl ions may cleave some ester bonds, acidic ions are quickly generated within the material, favoring acidic autocatalysis in bulk. On the surface, where the pH is buffered to 8, basic hydrolysis is considered negligible compared to enzymatic hydrolysis, which can cleave the chain at any point (β-ester bonds) [28], unlike non-enzymatic catalysis, which operates via an exocision mechanism (α-ester bonds) [19]. This means that for a commercial PLA with a molecular weight of around 40, 000 g/mol (72 g/mol per repeating unit), proteinase K is approximately 500 times more likely able to find the correct substrate (β-esters) than hydroxyl ions (OH^-) or hydronium (H_3O^+) ions are to find theirs (α-esters). This is why, in this study, we consider only two catalysts: proteinase K at the solid/liquid interface and H_3O^+ in bulk.

Our aim was to highlight the physical parameters that prevent PLA from degrading rapidly, despite its promising chemical structure for the living world. This is why the research hypothesis is primarily grounded in the premise that, during enzymatic catalysis, an entire segment of a polymer chain must disengage from its neighboring segments to effectively interact with the enzyme's active site. This suggests that the solid/liquid boundary is not as well defined as previously thought, indicating the existence of a semi-dissolved phase that possesses sufficient mobility to interact with the enzyme's active site at the material's surface.

The objective of this paper is to unify all the parameters influencing polyester hydrolysis into a single framework, proposing a coherent mechanism that encompasses both enzymatic and non-enzymatic hydrolysis. To achieve this, we first need to understand the interconnections between these parameters, specifically how they influence one another. In this study, the properties of nanochitin (NCh) are explored to introduce acidic species directly into the material bulk, enhancing acidic hydrolysis. Chitin, a structural polysaccharide derived from crustaceans and insects, was first identified by French chemist Auguste Odier in 1823 [34]. Exhibiting antimicrobial properties, chitin has found applications in food packaging [35], and its fungal inhibition and barrier properties have been studied in PLA/NCh samples [36, 37]. Recent advancements in chitin extraction and surface functionalization techniques have popularized NCh [38]. Recognized and processed by microorganism-derived enzymes, particularly marine-origin enzymes, chitin is widely regarded as an eco-friendly additive [39–41]. The choice of NCh as an additive was driven by several criteria: the additive had to be chemically modifiable to introduce acidic functionalities, eco-friendly, and improve material properties within the context of eco-design. For instance, mechanical reinforcement should serve as a "depolymerization-inducing" additive [42]. Carbohydrate-based substances, such as natural fibers [43, 44], and protein-based substances that trigger protease secretion [45], have shown promise. Among these, NCh have demonstrated good mechanical reinforcement in PLA [36, 46–48] and biodegradability [39, 44].

To achieve these objectives, various PLA formulations were meticulously prepared, taking into account several critical factors: the manufacturing method (either solvent or melt casting), the type of PLA used upon the D-content (whether amorphous or crystallizable), and the inclusion of additives that introduce acidic functionalities into the material. Different formulations were thereby developed, including non-functionalized NCh (NCh-HCl), and lactic acid-functionalized NCh (NCh-Lact). The capacity of these formulations to release acidic species was thoroughly assessed. Given that these nanocrystals are recognized as effective nucleation agents, we employed two types of PLA: amorphous and crystallizable. This approach was essential because crucial properties, such as the glass transition temperature (T_g), water absorption, and surface morphology, can be significantly influenced by the crystallization process. The sample hydrolysis was examined in the presence of proteinase K, a well-established enzymatic system known for its efficiency in rapidly depolymerizing PLA.

2. Materials and methods

2.1. NCh synthesis

Non-functionalized NCh (NCh-HCl), lactic acid-functionalized NCh (NCh-Lact) were prepared as described by Magnani *et al.* in 2022 [49]. The size of nanochitin was measured by Scanning Transmission Electron Microscopy (STEM). A drop of solution was deposited on a copper grid covered with a thin layer of carbon. After drying, images are taken under *a Hitachi SU8020* scanning electron microscope equipped with a transmitted electron detector, at a voltage of 30 kV. The functionalization was verified by FT-IR.

2.2. Acidic species releasing from NCh

Nanocrystals were immersed (0.2 mg/mL) in 3 mL of deionised water at 37 °C during 4 days. Then, each media was centrifuged at 20,000 g for 5 min to wash the nanocrystals. After two successive washes, the supernatant (2 ×1.5 mL) was retained, and the nanocrystals were freeze-dried. FT-IR analyses was performed on the nanocrystals, and the conductivity was measured on supernatant with *SI Analytics Lab 945* equipment.

2.3. Samples preparation

PLA 4060D and PLA 4032D were supplied by *NatureWorks*. According to the manufacturer, PLA 4060D contains 10 % of D-lactide and PLA 4032D contains 1.7 % of D-lactide. Both have a number average molecular weight (M_n) of approximately 70,000 g/mol (relative to GPC polystyrene calibration). The technical grade chloroform was supplied by Sigma Aldrich.

To perform solvent cast samples, PLA (amorphous PLA 4060D (10 % D-lactide) or crystallizable PLA 4032D (1.7 % D-lactide)) and NCh (mixture = 1.8 g) were solubilized under magnetic stirring in 30 mL chloroform. After adequate NCh dispersion (three hours), the solution was poured into a small crystallizer (diameter 7 cm). A larger crystalliser is turned upside down over the smaller one. The setup was placed on two layers of paper towels to slow chloroform evaporation over 10 days. Subsequently, films were placed under vacuum at 40 °C, and the temperature was increased by 5 °C every hour until reaching 110 °C. The samples are cooled to room temperature under vacuum. Detaching the films from the crystallizer required freezing the amorphous PLA films at −20 °C and scraping the edges. The films made with crystallizable PLA detached easily. Rectangles (2 cm×1 cm) were cut with a paper cutter (*Dahle - Professional guillotine paper cutter 533, 13 3/8 in* equipment).

To prepare melt cast samples, PLA and NCh were preliminary mixed by solvent casting in chloroform to protect nanocrystals prior to extrusion heat and films were dried under vacuum at 110 °C. Then, films were cut into small pieces (about 1 cm^2) before extrusion (*DSM Miniextruder 15cc*, 180 °C, 3 min at 30 rpm and 2 min at 60 rpm). Extruded formulations were cut into small pieces (about 3 mm), then dried in vacuum at 60 °C before compression molding (*Carver 4120 hydraulic press* equipment) at 180 °C during 5 min (1.4 g in mold (450 μm x 5 cm×5 cm), 2 min contact, 1 min 3 tons, 1 min 5 tons, 1 min 7 tons, degassing every 30 seconds). Rectangles (2 cm×1 cm) were cut with a paper cutter (*Dahle - Professional guillotine paper cutter 533, 13 3/8 in* equipment).

Several missing samples among those prepared by melt casting are

due to an insufficient quantity of nanochitins remaining for their preparation, due to technical reasons. To avoid introducing variability into the experimental design, we chose not to produce a new batch of nanochitins. For this reason, the experimental design results do not include any samples at 3 %: even the solvent-cast samples at 3 % were entirely removed from the experimental plan.

2.4. Immersion in (non)-enzymatic solution

First, samples were immersed in enzymatic solution (0.2 mg/mL proteinase K (Zellbio ZXB-06–107, 28,500 Da, activity > 30 U/mg), pH = 8.0 (TRIS HCl buffer 0.1 M)) at 37 °C for 4 days. Moreover, the enzymatic solution was changed every 24 hours to ensure constant enzymatic activity. In parallel, these formulations were also immersed under the same conditions but without any enzyme. After immersion, samples were cleaned with desionised water, then dried in oven under vacuum at 25 °C for 2 days. The mass loss and the molar mass loss were measured.

After this initial immersion in enzymatic solution, the samples (about 1 cm^2) were re-immersed under exactly the same conditions, but without the enzyme (only two replicate). Beforehand, the samples were dried overnight at 110 °C to remove any water that might have adhered during storage, and to ensure that no active enzymes remained on the sample surface prior to immersion in non-enzymatic solution. After immersion, samples were cleaned with desionised water, then dried in oven under vacuum at 25 °C for 2 days. The mass loss was measured.

To assess the effect of factors such as manufacturing, crystallization rate, type of PLA, NCh type and NCh weight%, on the measured response (mass loss or molar mass loss), we compared specific sample populations according to the method of Design of Experiments (DOE) by Taguchi procedure [50].

When oligomers are formed and reach a sufficient size to be soluble in the immersion media, they leave the material. This phenomenon is called "erosion" and is assessed by measuring the material mass loss. The mass of each sample was measured with analytical balance and was calculated with Eq. 1.

$$Mass_{loss} = \frac{Mass_{be} - Mass_{af}}{S} \quad (1)$$

With $Mass_{be}$ = sample mass before immersion (mg)

With $Mass_{af}$ = sample mass after immersion (mg)

With S = sample contact surface area with enzymatic solution, measured with a caliper

To assess the chain size and oligomers still present in the material, the molar mass was measured. Samples were analyzed by Gel Permeation Chromatography (GPC). GPC analysis was performed in tetrahydrofuran at 35 °C using an Agilent liquid chromatograph equipped with an Agilent degasser, an isocratic High Performance Liquid Chromatography (HPLC) pump (flow rate = 1 mL/min), an Agilent autosampler (loop volume = 100 µL, solution conc. = 2 mg/mL), an Agilent-DRI refractive index detector and three columns: a PL gel 10 µm guard column and two PL gel Mixed-D 10 µm columns (linear columns for separation of MW ranging from 500 to 10,000,000 g/mol of polystyrene (PS) used as standard). To evaluate the oligomer quantity inside the material, GPC curves have been integrated over the whole curve to take account of the presence of oligomers formed in the material, and calculate the M_n. All the molar masses are relative to PS calibration. The molar mass loss was calculated with Eq. 2.

$$Molar\ mass_{loss} = \frac{Mn_{be} - Mn_{af}}{Mn_{be}} \cdot 100\% \quad (2)$$

With Mn_{be} = M_n of sample before immersion measured by GPC (g/mol)

With Mn_{af} = M_n of sample after immersion measured by GPC (g/mol)

In order to highlight the impact of factors such as manufacturing, the PLA type, the crystallization rate, the NCh weight% and the NCh functionalization, on the mass loss and molar mass loss, the data were treated in the manner of a design of experiment. Table S1 shows which sample populations were compared for each factor.

We name the response y as mass loss or molar mass loss. y and e are defined as the mean response and standard deviation respectively, of the formulation obtained from the responses of the replicates (y^1, y^2 and y^3). Then, for each formulation, two other responses are calculated: $y^- = y - e$, and $y^+ = y + e$. To summarize, we transform y^1, y^2 and y^3 into three other values y^-, y and y^+, whose y means are equal and where y is always centered between y^- and y^+. Values are shown in tables S2 and S3.

To assess the effect of factors such as manufacturing, crystallization rate, type of PLA, NCh functionalization and NCh weight%, on the measured response, we compared specific sample populations according to the method of Design of Experiments (DOE) by Taguchi procedure [50]. For example, the effect of manufacturing was evaluated by comparing amorphous solvent cast samples (code Sa…) and amorphous melt cast sample (code Ma…).

To assess the manufacturing effect, simply compare Y_{Sa} and Y_{Ma}, where Y_{Sa} is the average of the y responses of samples with code Sa and Y_{Ma} is the average of the y responses of samples with code Ma. The standard error of Y_{Sa} is calculated with Eq. 3. With the same principle, it is possible to calculate the effect of crystallization rate, the %D-Lactide, the functionalization of NCh and the NCh weight%.

$$St.error\ of Y_{Sa} = Y^+_{Sa} - Y_{Sa} = Y_{Sa} - Y^-_{Sa} \quad (3)$$

Where Y_{Sa} is the average of y responses of Sa population samples.

Where Y^+_{Sa} is the average of y^+ responses of Sa population samples. It's the high average.

Where Y^-_{Sa} is the average of y^- responses of Sa population samples. It's the low average.

2.5. Samples characterization

2.5.1. Scanning electron microscopy

The material surface morphology was assessed qualitatively by Scanning Electron Microscopy (SEM) before and after hydrolytic degradation. The pictures were taken on the surface (top view) and on the cross section (edge view) of samples with 0 and 2 % of NCh-Lact. For the cross section, the samples were immersed in liquid nitrogen for a few minutes and then manually fractured. Then, a 5 nm tungsten deposit was sputtered onto the samples using a *Leica ACE 600* equipment. Pictures were acquired in a *Hitachi SU8020* scanning electron microscope, using SE(L) and SE(U) as Secondary Electron detectors, at voltages of 3 kV and 5 kV.

2.5.2. Water uptake

Squares immersed in 5 mL TRIS-HCl buffer 0.1 M (pH = 8.0) during 4 days at room temperature. After immersion, the samples were immediately wiped with paper then weighed. Then, samples were dried for 48 hours under vacuum at room temperature, and then at 80 °C for 48 hours. After drying, the samples were weighed again. The water uptake (% by weight) in the material was calculated using Eq. 4.

$$Water\ uptake = \frac{Mass^{be}_{dry} - Mass^{af}_{dry}}{Mass^{be}_{dry}} \cdot 100\% \quad (4)$$

With $Mass^{be}_{dry}$= sample mass before drying

With $Mass^{af}_{dry}$ = sample mass after drying

2.5.3. Differential Scanning Calorimetry

The chain mobility (and thus their accessibility for the enzyme) in the amorphous region was assessed by measuring the T^s_g on samples of about 5 mg immersed in TRIS-HCl buffer 0.1 M pH= 8.0 during 4 days at room temperature using *TA DSC Q2000* equipment. The DSC were

carried out under N_2 atmosphere at 20 °C/min in hermetic pan. The soaked sample was put in hermetic pan with 5 µL of buffer. In the reference pan, 5 µL of buffer was put also. In parallel, the dry material T_g was measured in the same conditions, but without buffer in the pan. Moreover, the crystallinity rate was calculated by DSC (10 °C/min, first heat cycle) with Eq. 5.

$$Cryst. = \frac{\Delta m - \Delta c}{\Delta_m^{100\%}} \cdot 100\% \quad (5)$$

With Δm = melt enthalpy measured by DSC (J/g)
With Δc = cold crystallisation enthalpy measured by DSC (J/g)
With $\Delta_m^{100\%}$ = melt enthalpy of pure crystal of PLA (93 J/g) [48]

2.5.4. X-ray diffraction

The chain accessibility in the crystalline region was assessed by XRD. XRD analysis was carried out with a Panalytical Empyrean diffractometer with an area detector operating under Cu Kα radiation (1.5418 Å, 40 kV, 40 mA). By XRD, the crystallinity rate calculation was inspired from the method of Hsieh *et al.* in 2020 [51] (Fig. S1).

3. Results and discussion

3.1. Identifying early trends: Immersion in enzymatic solution

PLA/NCh samples were prepared by melt casting or solvent casting in the presence of functional (NCh-Lact) and non-modified NCh (NCh-HCl) [49] (Table 1). The average NCh-HCl length was estimated at 215 ± 50 nm and that of NCh-Lact was estimated at (226 ± 46) nm (based on 11 representative samples) using Transmission Electron Microscopy (TEM) (Fig. S2). The Fourier Transform-Infrared Spectroscopy (FT-IR) confirmed the successful NCh functionalization and show the NCh-lact capacity to release acid species unlike NCh-HCl (Fig. S3), where the structure of nanocrystals were detailed.

The PLA/Nch sample thickness was measured by Scanning Electron Microscopy (SEM) after cryofracture on samples with 0 or 2 % of NCh-Lact, and was 418 ± 56 µm. The sample mass before immersion was 106 ± 9.7 mg (Fig. S4).

Fig. 2 **A** depicts the sample visual characteristics (only the first replicate) before and after immersion in enzymatic solution. Following immersion, the samples exhibited an increase in opacity. Previous studies have investigated the evolution of opacity in these PLA-based materials, revealing that several factors contribute to this phenomenon, including: (a) light scattering due to water presence [52]; (b) the formation of degradation products during hydrolysis [53]; (c) the development of surface roughness due to the emergence of voids during degradation [53, 54]; and (d) an increase in the polymer matrix crystallinity [55]. Notably, our samples were dried prior to immersion, and the crystallinity remained unchanged throughout the immersion process (approximately 0 % or 45 % as measured by Differential Scanning Calorimetry (DSC) [56] and confirmed by X-Ray Diffraction (XRD) (Fig. S1) [51]. This suggests that the observed surface opacity primarily results from the presence of degradation products within the material, along with potential alterations in surface roughness induced by enzymatic degradation.

Fig. 2 **B** and **C** illustrate the changes in mass loss and molar mass loss as a function of the NCh concentration within the polymer matrix, as well as their respective functionalization. Notably, no significant alteration in mass or molar mass were observed in samples immersed in the absence of proteinase K. Overall, the NCh incorporation resulted in increased mass loss and molar mass reduction, with a pronounced effect in samples prepared via solvent casting. This finding suggests that the solvent casting method facilitates bulk degradation, particularly for NCh-Lact, thereby enhancing the polymer's susceptibility to hydrolytic processes.

Fig. 2 **D** consolidates the mass loss data, elucidating the primary factors influencing the hydrolytic degradation of PLA in the presence of enzymes. The dominant factors identified include the manufacturing method, the crystallization rate, and the NCh weight%. Notably, the percentage of D-lactide within the PLA matrix emerges, alone, as a negligible factor within the studied range (<10 % D-lactide), although proteinase K is unable to hydrolyze D-unit of PLA [28]. Furthermore, the NCh functionalization with lactic acid proves to be significant only when the samples are produced via solvent casting.

Fig. 2 **E** aggregates the data on molar mass loss. Similar to the trends observed in mass loss, the primary factors influencing molar mass loss are the manufacturing method the crystallization rate, and the NCh weight%. The corresponding GPC curves are presented in Fig. S5.

The most significant trends observed include the influence of the manufacturing method (solvent versus melt casting), the crystallinity rate (well-documented in the literature[57, 58]), and the presence of NCh. The NCh incorporation facilitates greater mass loss, even when the molar mass remains constant during immersion. This suggests that degradation occurs primarily at the surface rather than in the bulk, particularly in samples prepared via melt. Consequently, NCh enhances bulk degradation through acidic catalysis—an effect that is amplified in samples prepared by solvent casting or those featuring functionalized NCh. Furthermore, it also promotes surface degradation via enzymatic catalysis. Given that samples produced through solvent casting demonstrate more advanced bulk degradation, they appear to be more susceptible to non-enzymatic hydrolysis compared to their melt-cast counterparts. Notably, NCh-Lact enhances acidic hydrolysis by releasing acidic species (Fig. S3); however, the NCh specific role in enhancing enzyme catalysis remains to be elucidated.

To advance our understanding, we aim to (a) investigate why certain samples exhibit greater "accessibility" to the enzyme, (b) identify the key parameters through which manufacturing methods and the presence of NCh-Lact enhance PLA hydrolysis, (c) discern why the NCh impact is more pronounced in samples prepared by solvent casting, and (d) demonstrate that solvent-cast samples can undergo hydrolysis without the presence of an enzyme, unlike those produced by melt casting.

3.2. Identifying the most accessible samples for the enzyme

The specific surface area is widely recognized as a crucial factor in the degradation processes of materials [30]. In this study, we qualitatively assessed the specific surface area using SEM on both the surface and cross-section of cryo-fractured samples (Fig. 3 and 4). Notably, samples immersed without proteinase K exhibited no significant changes in surface morphology (Fig. S5 and S6).

Fig. 3 displays SEM images of amorphous PLA samples, taken before immersion (cross-section) and after immersion (both cross-section and surface). Collectively, images indicate that the degraded samples exhibit a "sponge-like network structure," a phenomenon previously observed by Kurokawa *et al.* in 2008 [59]. Importantly, the enzyme does not merely act on the surface; it penetrates the material, creating a network of galleries at varying depths. While non-enzymatic degradation primarily occurs within the bulk, enzymatic degradation is characterized by a perforation mechanism, where hydrolysis occurs at the water/-material interface and can extend into the material due to the galleries formed by the enzyme (deep perforation). It is essential to note that even when degradation is confined to the surface (as exemplified by the MaPLA sample) the enzyme continues to operate via a perforation

Table 1
Sample codes. Each formulation was prepared in 3 replicates. "a" = amorphous PLA and "c" = crystallizable PLA.

Manufacturing	PLA	NCh	NCh weight
S = Solvent casting	a = 10 % D-lactide	H = NCh-HCl	0 % = PLA
M = Melt casting	c = 1.7 % D-lactide	L = NCh-Lact	1 %
			2 %
			3 %

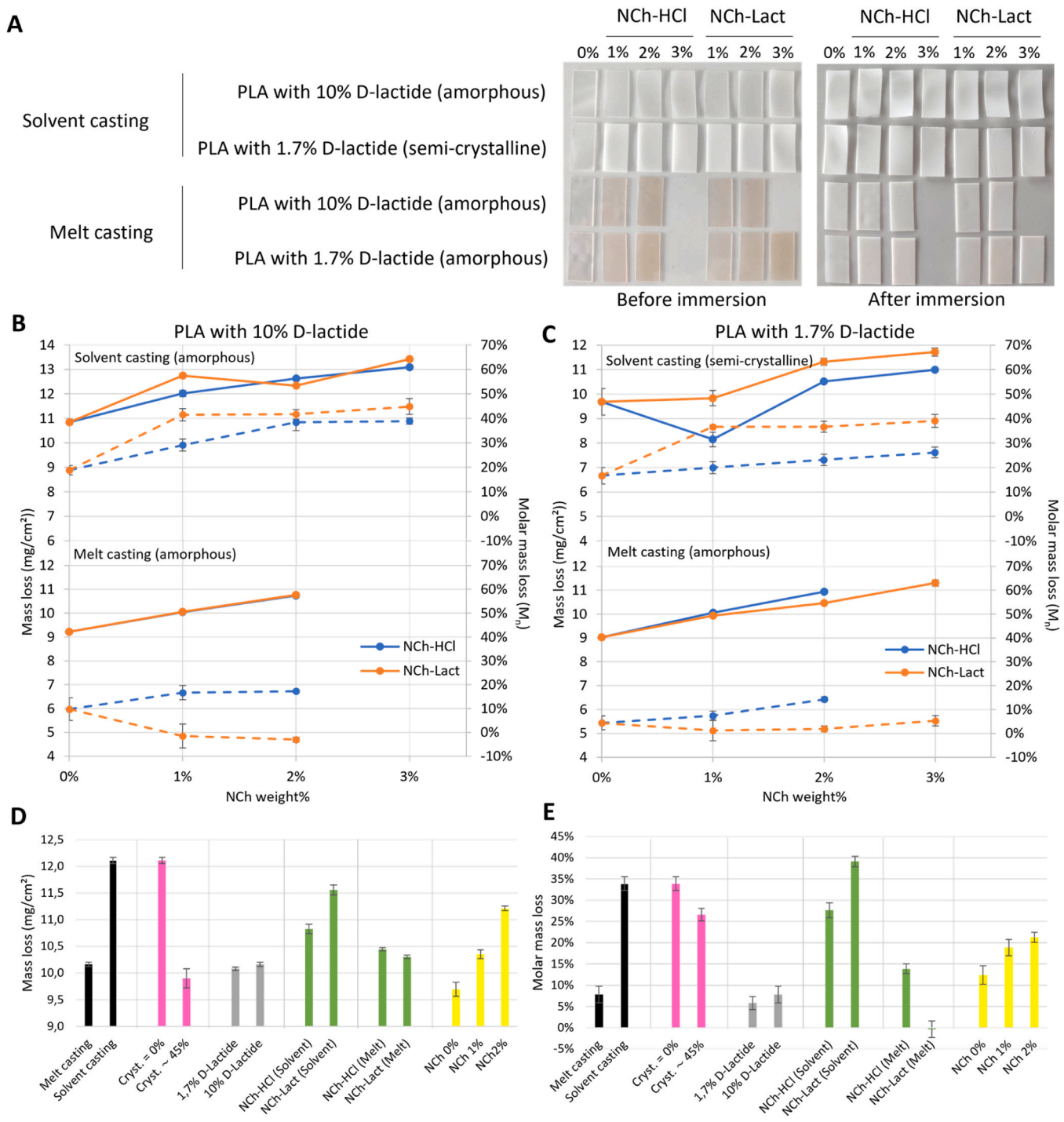

Fig. 2. Immersion in enzymatic solution (0.2 g/L proteinase K, pH = 8.0) at 37 °C during 4 days. A Sample visual aspects before and after immersion (only first replicate); Mass loss (solid lines) and molar mass loss (dotted lines) depending on the NCh weight% of **B** 10 % D-lactide PLA samples and of **C** 1.7 % D-lactide PLA samples; Design of experiment [50] : effects of manufacturing (black), crystallization rate (pink), PLA type (gray), NCh type (green) and NCh weight% (yellow) on **D** the mass loss and on **E** the molar mass loss.

mechanism (superficial perforation).

As illustrated in Fig. 3 the NCh effect and the manufacturing method on the enzymatic degradation of PLA is pronounced. Solvent casting, in conjunction with the presence of NCh, significantly facilitates the enzyme's ability to penetrate the material. This enhanced perforation likely results from increased chain accessibility, allowing the enzyme to interact more rapidly with the polymer chains and thereby accelerating the degradation process.

Fig. 4 presents SEM images of crystallizable PLA samples. In the case of amorphous materials (McPLA and McL2%), the results mirror those observed in MaPLA and MaL2% (Fig. 2) with the perforation mechanism remaining primarily superficial. However, when transitioning from amorphous (SaPLA in Fig. 3) to semi-crystalline (ScPLA in Fig. 4), the enzyme's perforation appears to be hindered (absence of galleries). This reduced accessibility arises from the significantly lower chain mobility within the crystalline regions compared to the amorphous domains, which fosters interaction between the polymer chains and the enzyme [24, 60]. Notably, the introduction of 2 % of NCh-Lact (ScL2%

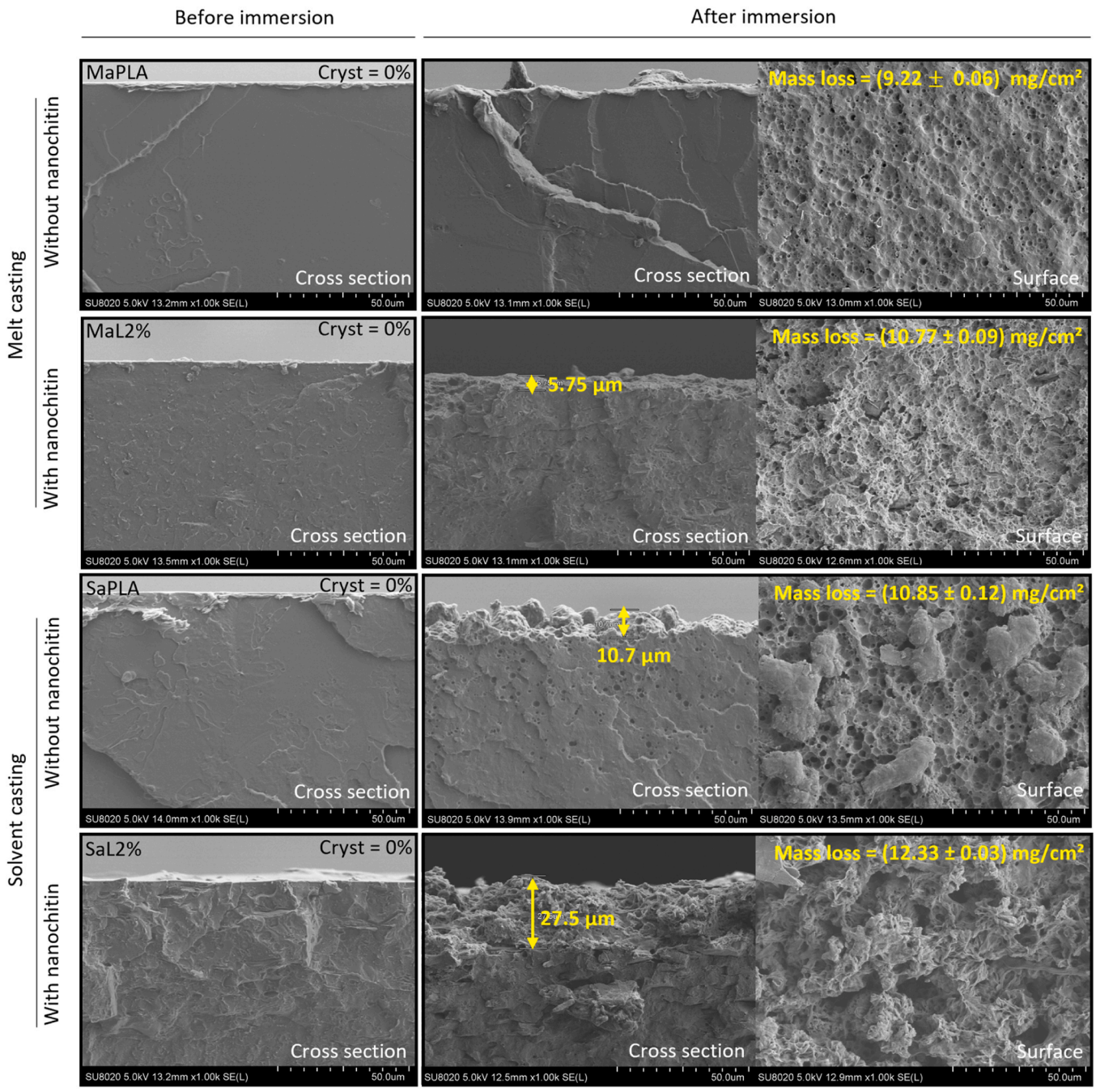

Fig. 3. Immersion in enzymatic solution (0.2 g/L proteinase K, pH = 8.0) at 37 °C during 4 days: Scanning Electron Microscopy (SEM) pictures of samples prepared with amorphous PLA (containing 10 % D-lactide) before (cross section) and after immersion (cross section and surface). The depth perforation is shown in yellow (µm), and the mass loss is reminded. Sample codes are shown in Table 1. SEM pictures of the samples surface before immersion are shown in Fig. S6. The crystallinity rate (Cryst.) was measured by Differential Scanning Calorimetry (DSC).

compared to ScPLA in Fig. 4) markedly alters the surface and cross-sectional morphology prior to degradation, as NCh serves as nucleation points [61] . This enhancement of specific surface area results in a greater quantity of enzyme adsorption onto the material [30] . Before immersion, the ScL2% sample surface appears highly irregular, featuring deep chasms that likely contribute to the significant perforation depth (124 µm), in contrast to other samples which exhibit depths of less than 30 µm.

It is crucial to emphasize that perforation depth alone does not dictate the measured mass loss. For instance, the SaL2% sample (Fig. 3) shows a perforation depth of 27.5 µm, correlating with a mass loss of 12.33 ± 0.03 mg/cm², while the ScL2% sample (Fig. 4), exhibiting a perforation depth of 124 µm, has a mass loss of 11.33 ± 0.15 mg/cm². This observation suggests that other hydrolytic mechanisms, such as non-enzymatic degradation, are facilitated within the amorphous regions.

3.3. *Key parameters in enzymatic and acidic hydrolysis*

After initial immersion in enzymatic solution, the samples were re-immersed under exactly the same conditions, but without enzyme (only two replicate) during 4 days, to highlight which samples are able to continue degradation without enzymes (Fig. S8).

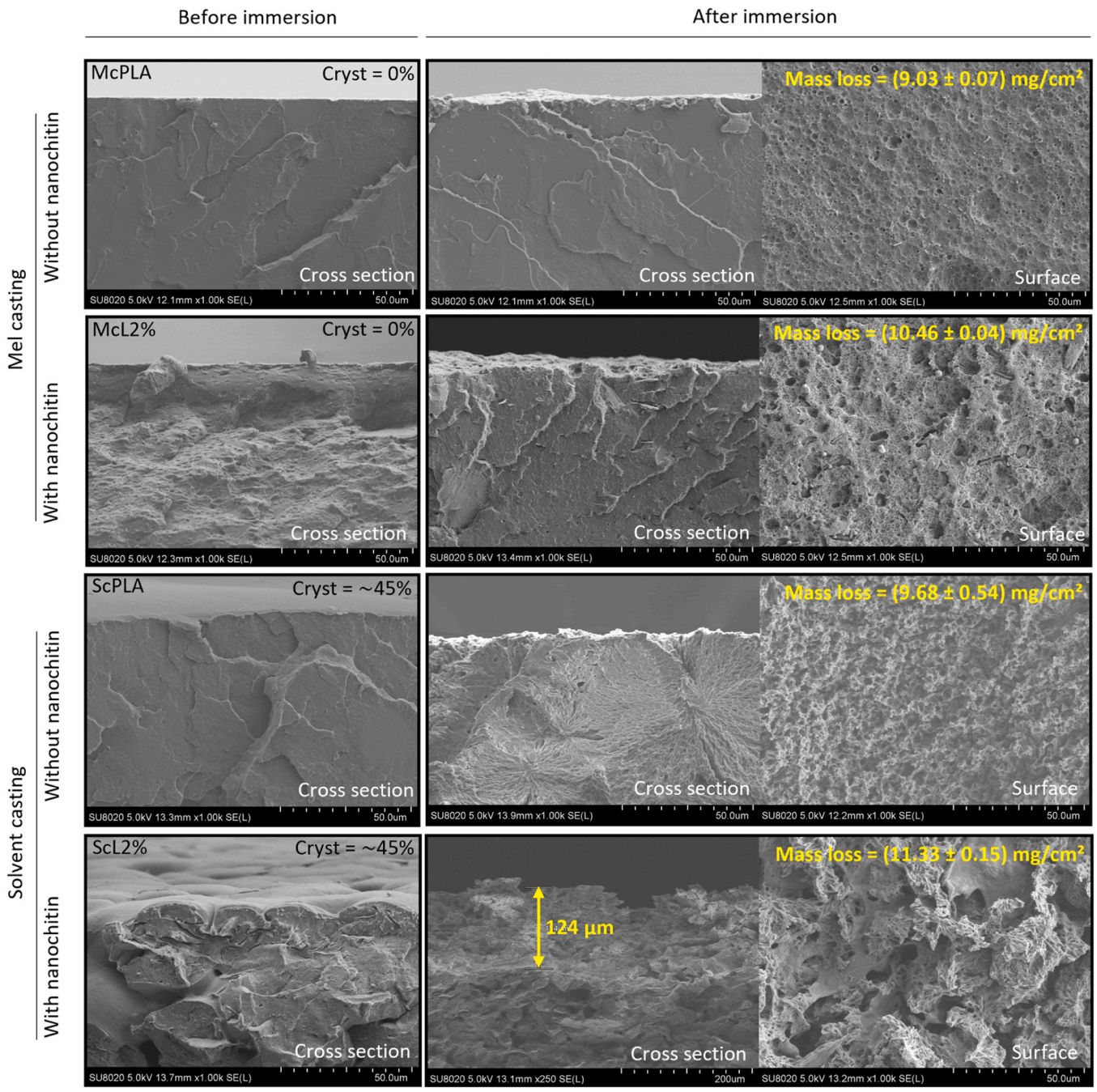

Fig. 4. Immersion in enzymatic solution (0.2 g/L proteinase K, pH = 8.0) at 37 °C during 4 days: Scanning Electron Microscopy (SEM) pictures of samples prepared with crystallizable PLA (containing 1.7 % D-lactide) before (cross section) and after immersion (cross section and surface). The depth perforation is shown in yellow (µm), and the mass loss is reminded. Sample codes are shown in Table 1. SEM pictures of the samples surface before immersion are shown in Fig. S7. The crystallinity rate (Cryst.) was measured by Differential Scanning Calorimetry (DSC).

3.3.1. Water uptake

The findings presented in Fig. 2 suggest that NCh facilitates the entrapment of oligomers within the material, as indicated by the decrease in the M_n, which is characteristic of non-enzymatic bulk degradation. This degradation pathway is favored when water readily diffuses through the material, enhancing water uptake [20]. To elucidate the factors influencing water uptake in various PLA/NCh formulations, we measured the water absorption by weight before any degradation. The study of the influence of pH on water uptake was not considered, as it is in fact the ionic force of the media that is involved, and not the pH itself [62].

Initially, Fig. 5 A illustrates water uptake as a function of sample formulation. The manufacturing method (Sa samples vs. Ma samples) and the crystallinity rate (Sa samples vs. Sc samples) emerge as the most significant determinants. This may be due to the fact that the hydrophilic carbonyl groups "point" towards the surface when the solvent evaporates during solvent casting sample preparation, due to the humidity in the air. The surface of these samples is then more hydrophilic than their melt-cast counterparts, facilitating plasticization of the water and thus interaction with the enzyme. Furthermore, the NCh functionalization and its concentration within the material exert a substantial influence on water uptake, particularly in samples produced via solvent casting. Specifically, samples prepared by solvent casting that incorporate NCh-Lact demonstrate higher water absorption, which correlates

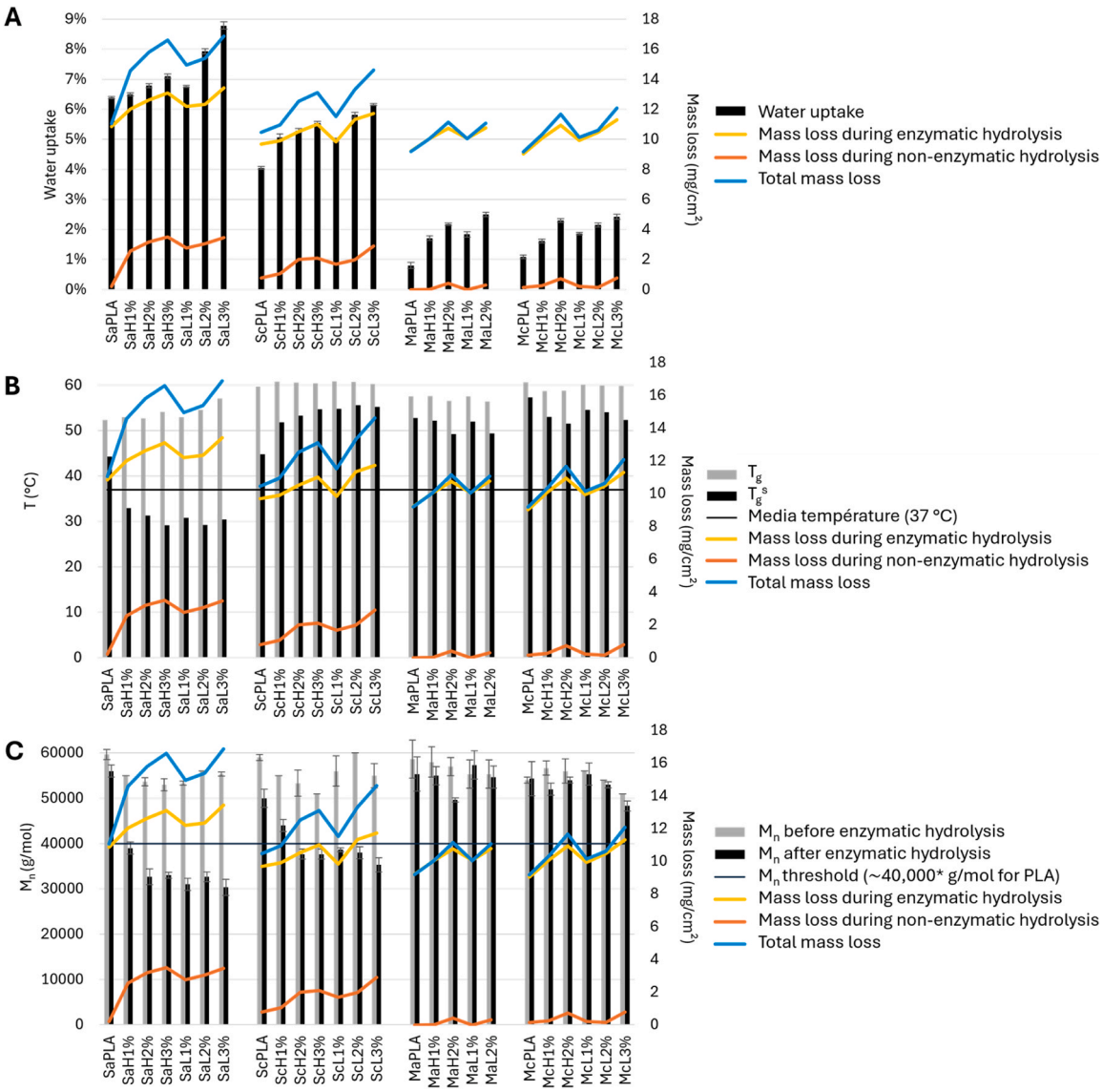

Fig. 5. Key parameters influencing the enzymatic and non-enzymatic hydrolysis of polyesters. The sample codes are shown in Table 1. The samples were first immersed in enzymatic solution (0.2 g/L proteinase K, pH = 8.0, at 37 °C during 4 days), and then re-immersed under the same conditions, but without the enzyme. A The material water uptake before any degradation; B The soaked material glass transition temperature (T_g^s) before any degradation; C The molar mass, which plays a pivotal role in non-enzymatic hydrolysis through the exocision mechanism. These findings suggest the existence of a physico-chemical threshold state that governs the onset of non-enzymatic hydrolysis: for polylactide (PLA), only samples with a molar mass below approximately 40,000 g/mol (*relative to GPC polystyrene calibration) are capable of enzyme-free hydrolysis.

with enhanced degradation performance (Fig. 2). These findings underscore the advantages of functionalization: the introduction of acidic functionalities enhances the material's hydrophilicity, promoting greater water absorption and subsequently improving degradation. It is well established that water acts as a plasticizer, further facilitating this process [63]. Thus, NCh indirectly enhances the chain accessibility of the amorphous region through water-induced plasticization.

Secondly, as indicated in Fig. 5 A, water uptake alone does not fully account for the observed differences in degradation rates. For instance, the Sc samples and the M samples exhibit similar enzymatic degradation profiles despite significant disparities in water uptake. This suggests that enzymatic degradation is predominantly influenced by the chain mobility; sufficient chain mobility is necessary for effective interaction with the enzyme's active site. Therefore, it is essential to examine the soaked material T_g to further understand these dynamics.

3.3.2. *Glass transition temperature of soaked material (T_g^s)*

The chain accessibility of the amorphous region was evaluated through the T_g of the soaked material (T_g^s), by DSC (Fig. S9).

Fig. 5 **B** presents the T_g of non-degraded samples, both unsoaked (T_g) and soaked material (T_g^s). Samples prepared by solvent casting (Sa…) exhibit better chain mobility and, consequently, greater chain accessibility than those produced by melt casting. This difference explains the more efficient perforation observed in samples prepared by solvent casting. Additionally, as expected, the crystallinity rate significantly influences the T_g: amorphous samples (Sa…) have a lower T_g than their semi-crystalline counterparts (Sc…). Notably, while NCh has no significant effect on the T_g, it does influence the T_g^s.

Fig. 5 **B** clearly shows that the amorphous samples prepared by solvent casting (Sa samples) and immersed in the buffer exhibit a T_g^s lower than the temperature of the surrounding media (37 °C). Consequently, the enzyme interacts with chains capable of sliding each other, allowing translational movement. At the material surface, it is

reasonable to conclude that the enzyme operates in a semi-dissolved state on the Sa samples, which made digging the gallery easier into the material. These findings are consistent with the SEM images (Fig. 3) that demonstrate the enzyme's perforation: chain accessibility is enhanced when samples are prepared by solvent casting. Furthermore, the T_g^s elucidates how NCh enhances enzyme penetration. It is worth pointing out that the T_g recorded by DSC corresponds to an average value for the entire analyzed sample. If a reduction is observed for the T_g^s, it means that the polyester chains at and underneath the top-surface are more "plasticized" by water molecules leading to a "local' T_g appearing at lower temperature with resptect to the values that would have been measured lower in the core of the sample. Therefore, the reduction of the overall ("average") T_g^s as recorded by DSC for the entire sample does not represent the reduction of the T_g^s at the interface with water, which is most likely more pronounced.

To our knowledge, the T_g^s has not been considered an essential factor in the hydrolysis of materials. Until now, research has focused primarily on the T_g of dry materials. However, as shown in Fig. 5 **B** an additive like NCh may not affect the dry material T_g—thus preserving mechanical properties-but may have a significant impact on the soaked material T_g^s. This finding illustrates the potential to enhance both the mechanical properties and degradation characteristics of a material, challenging the long-standing notion that these attributes are antagonistic in eco-design approaches. Ultimately, the T_g^s emerges as a central key parameter in polyester hydrolysis. More broadly, the T_g^s is crucial to all enzymatic polymer degradation processes. Indeed, the T_g, which quantitatively reflects the mobility of polymer chains, is a universal property of all polymers. The mobility of chains located at the outermost surface of an immersed material will inevitably differ from that of chains at the material/air interface. Consequently, the enzyme perceives T_g^s, never the T_g of the dry material. It is important to note, however, that highly hydrophobic materials may not experience such a decrease in T_g^s upon immersion, as they cannot benefit from effective plasticization by water, thereby limiting the enzyme penetration depth. Therefore, when considering biodegradation at room temperature, the importance of T_g^s relative to T_g will be much more pronounced in high T_g matrices such as PLA or polyethylene terephthalate (PET) [64]. Conversely, polyesters with a low T_g, such as polybutylene adipate terephthalate (PBAT) or polybutylene succinate (PBS), are less constrained by their T_g^s because their low T_g already allows for excellent biodegradation [65].

3.3.3. Molar mass

The central key parameter in the non-enzymatic hydrolysis of polyesters is molar mass, specifically the chain end density. Acidic catalysis operates via an exocision mechanism, where chain ends serve as the primary reactants. Additionally, a higher chain-end density enhances chain mobility, which in turn increases water permeability.

As highlighted by Tsuji and Hyon in the 90 s [66–68], non-enzymatic hydrolysis accelerates significantly once the M_n approaches approximately 40,000 g/mol for PLA (relative to GPC polystyrene calibration). In our experiments, samples that attained this threshold during enzymatic degradation (referred to as Sa samples) were subsequently able to degrade further in the absence of enzymes. By contrast, samples prepared by melt casting, which primarily experienced surface degradation during enzymatic hydrolysis, exhibited minimal degradation without enzymatic assistance. This observation clearly indicates that enzymatic hydrolysis occurs at the solid/liquid interface of the material, whereas acidic hydrolysis takes place within the material bulk. Furthermore, these findings suggest that enzymatic hydrolysis can serve as a precursor to initiate non-enzymatic hydrolysis.

3.4. Key parameters interconnections

Fig. 6 illustrates the interconnections among various parameters influencing both enzymatic and acidic hydrolysis of polyesters. We have delineated the effects of solvent casting and the presence of NCh on the parameters evaluated either directly or indirectly. These parameters may facilitate the interaction between the enzyme and PLA at the material scale, enhance the enzyme-PLA interaction at the enzymatic scale, or promote non-enzymatic bulk degradation at the molecular scale. The degradation types, highlighted in yellow, include both non-enzymatic (bulk) and enzymatic (superficial or deep perforation). Ultimately, our output encompasses mass loss and molar mass loss, where the phenomenon of erosion refers to the reduction of oligomers to a size that allows solubility in the media, thereby contributing to mass loss.

Regarding the influence of solvent casting method, our results indicate that the manufacturing method (solvent vs. melt casting) is the most significant factor affecting the mass loss of materials immersed in enzymatic solution. Fig. 6 elucidates the physico-chemical parameters through which solvent casting enhances the hydrolytic degradation of PLA. On one hand, the solvent casting method facilitates crystallization,

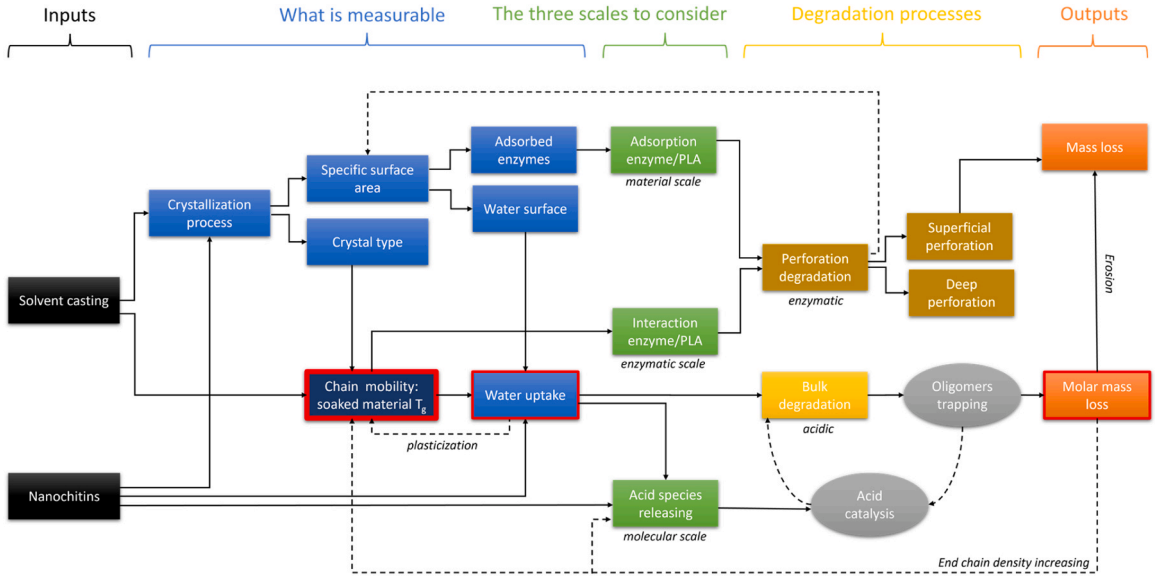

Fig. 6. Flux diagram: physico-chemical parameters induced by solvent casting and NCh in polyester hydrolytic degradation, to highlight the complexity of their relationship. Each arrow illustrates the influence of each parameter on the others. The glass transition temperature of soaked material (T_g^s), which reflects chain mobility, is the only parameter that directly influences enzyme/PLA interaction. All other parameters can be considered as means of varying the T_g^s.

which can reduce the degradation rate, as crystalline regions are less accessible and thus less mobile, limiting interaction with the enzyme's active site. Conversely, solvent casting substantially improves the accessibility of amorphous chains (as indicated by the T_g^s) effectively outweighing the adverse effects of crystallization on hydrolytic degradation. Moreover, crystalline phases within the matrix tend to confine the chains of the amorphous phase, restricting their mobility and increasing the material's T_g [27]. It is reasonable to assume that the influence of crystals on T_g^s follows similar mechanisms. However, in restricted amorphous regions between crystalline lamellae, water may have a reduced effect on chain mobility due to the presence of crystals, which partially immobilize multiple chain segments in these regions.

Regarding the NCh influence, it enhances both enzymatic and non-enzymatic hydrolysis of PLA by operating across all levels of the hydrolytic degradation process: material, enzymatic, and molecular scales. At the material scale, NCh increases the specific surface area, particularly when acting as nucleation points, thereby statistically elevating the frequency of hydrolytic reactions occurring simultaneously. Additionally, the presence of NCh promotes the crystalline α' form of PLA, which is more susceptible to hydrolysis than the α form (Fig. S10) [69, 70].

Furthermore, NCh enhances the material water uptake, facilitating two types of catalysis. [1] The increased water uptake enables the enzyme to create deeper galleries within the material. This effect is primarily attributed to the plasticizing action of water on PLA, which enhances chain mobility and thus facilitates enzyme perforation. The galleries formed contribute to a greater specific surface area, thereby

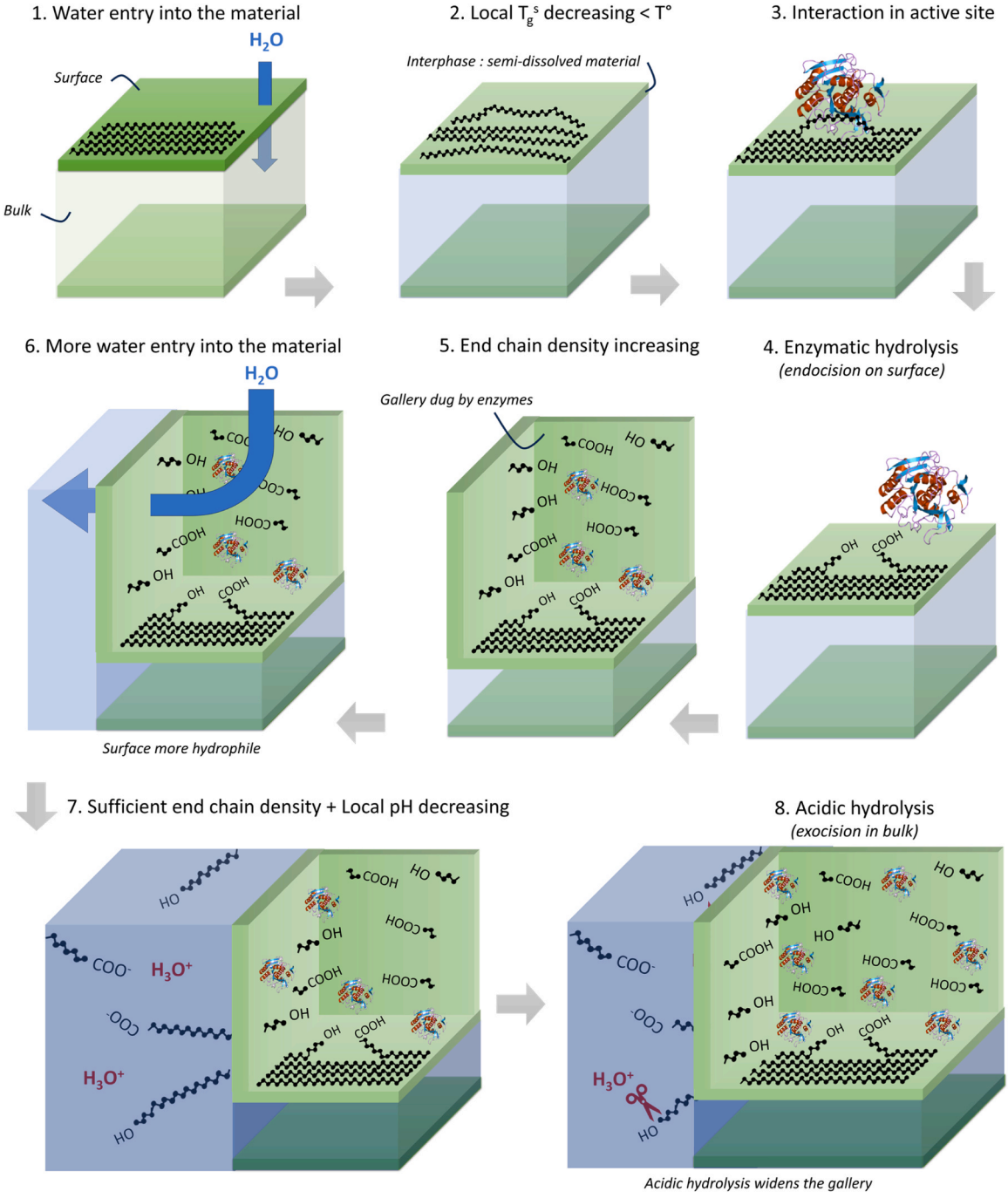

Fig. 7. Polyester enzymatic hydrolysis mechanism: how key parameters intervene in the hydrolysis of a polyester, and how these key parameters enable enzymatic hydrolysis (endoenzyme) on the surface to initiate acidic hydrolysis in bulk.

benefiting both enzymatic and non-enzymatic hydrolysis. This observation explains the lack of degradation in samples absent of enzymes, as the galleries created by the enzyme promote non-enzymatic hydrolysis. [2] From a chemical hydrolysis perspective, NCh facilitates higher water absorption into the material, especially when functionalized with lactic acid. The water present in the material (augmented by the galleries formed by the enzyme) hydrolyzes the NCh-Lact surface, releasing lactic acid (Fig. S3) that becomes trapped within the material. This localized acidity catalyzes hydrolysis, resulting in the formation of oligomers and promoting acid autocatalysis of PLA.

Chain mobility emerges as a central parameter in exhibiting the most connections to other parameters and comprising two critical positive feedback loops: water uptake via plasticization and molar mass loss due to increased chain-end density. Consequently, it is essential to consider water uptake and molar mass as key parameters, as they are intrinsically linked to the soaked material T_g^s. The relationship between T_g and T_g^s is closely linked to water uptake: the greater the material's ability to absorb water, the more T_g^s deviates from T_g. However, this relationship is also influenced by the surrounding temperature. As the temperature increases, chain mobility increases, facilitating higher water uptake, which in turn further enhances chain mobility.

Lastly, local pH should also be regarded as a significant factor in the non-enzymatic hydrolysis of polyester. However, local pH is directly influenced by both water uptake and molar mass. Therefore, the effects of local pH will manifest through those of water uptake and molar mass loss. If significant quantities of acidic species are incorporated into the matrix, for example through the addition of specific additives, then local pH should be regarded as an additional key parameter.

3.5. Mechanism

Based on the comprehensive information gathered in this work, we propose a coherent mechanism that highlights the key parameters involved in the hydrolysis of a polyester, illustrated in Fig. 7. This mechanism encompasses both enzymatic (endoenzyme) and non-enzymatic (H_3O^+) hydrolysis of polyester, illustrating how enzymatic hydrolysis can initiate non-enzymatic hydrolysis.

For enzymatic hydrolysis to occur, the T_g^s must be lower than the media temperature (step 2), facilitated by water uptake (step 1). However, the assumption is made that the chains at the surface are always sufficiently solvated (step 3) to undergo hydrolysis, even when the T_g^s exceeds the media temperature. In essence, the local T_g^s is the critical parameter in this context (step 3). Subsequently, the endoenzyme hydrolyzes the mobile chains (step 4), resulting in the production of an alcohol and a carboxylic acid functional group. This enzymatic action creates galleries (step 5) with increasingly hydrophilic walls, leading to enhanced water uptake in the material (albeit locally), which further promotes chain mobility and, consequently, enzymatic hydrolysis (step 6). For significant acidic hydrolysis to occur, a sufficient chain-end density must be achieved (approximately 40,000 g/mol for PLA), as the chain ends serve as the reactants. Additionally, the local pH must be acidic, which is closely related to chain-end density through the presence of carboxylic acid groups (step 7). Ultimately, acidic hydrolysis proceeds, releasing lactic acid and resulting in increased acidity and chain mobility (step 8), thereby triggering autocatalysis.

This mechanism underscores a central parameter: chain mobility linked to related chain-water interactions with the concomitant decrease of local T_g^s and the water-soaked polymer interface. In enzymatic hydrolysis, the catalyst is relatively large, necessitating an entire segment of a chain disengage from neighboring chains to interact with the enzyme's active site. Conversely, in acidic catalysis, chain mobility becomes a less critical factor, as the reactions occur on a molecular scale. The limiting stages of the proposed mechanism are steps 2 and 7.

4. Conclusion

Understanding the enzymatic depolymerization of plastics is crucial for enhancing biodegradability and facilitating enzymatic recycling. In this pursuit, we investigated the influence of specific parameters—such as the manufacturing method, type of PLA, and the addition of acidic species on the depolymerization of a polyester during both enzymatic and non-enzymatic degradation.

This study underscores the importance of considering these two types of degradation concurrently. It is increasingly untenable to study the enzymatic hydrolysis of a material without accounting for non-enzymatic hydrolysis. Eventually, the measured mass loss reflects both types of catalysis, rather than solely enzymatic hydrolysis. Consequently, enzymatic degradation rates are often overestimated in literature. Enzymatic hydrolysis is highly sensitive to the local soaked material T_g^s, while non-enzymatic hydrolysis is primarily influenced by chain-end density and local pH in the bulk. In summary, the key parameters deemed most relevant and impactful on polyester hydrolysis are the soaked material T_g^s, which is closely linked to water uptake, and the local pH in bulk, influenced by acidic species from additives or end-chain carboxylic acids.

Ultimately, this study demonstrates that only the local chain mobility in the enzyme vicinity is crucial. Other parameters discussed in the literature do not directly affect the degradation rate; instead, they influence chain mobility, which in turn governs the degradation rate. This study elucidates the detailed mechanism of hydrolytic degradation of polyesters, revealing critical intermediate steps that control the breakdown process.

The chain mobility "perceived" by the enzyme *(i.e.*, local mobility), as revealed in our study, could be the key factor underlying the competition between the amorphous and crystalline phases. The mobility of the chain encountered by the enzyme may be the alone determining parameter, regardless of whether the chain is located in the crystalline or amorphous phase. This would unify the degradation kinetics of both phases under a single model.

Our study complements the valuable work of enzymologists. For example, it would be interesting to design enzymes that require only short chain segments to enter their active site. Optimizing such enzymes, which would necessitate the movement of smaller chain segments, would reduce the energy required to achieve the desired mobility, enabling catalysis to occur at lower temperatures.

By comprehending the hydrolysis mechanism of polyesters and understanding how this newly identified key parameter operates, polymer researchers can direct their efforts toward optimizing this aspect, enabling the rapid and efficient design of new and more eco-friendly materials. The significant reduction in the number of parameters allows for the development of a simplified kinetic model, wherein the enzyme operates in a semi-dissolved media. Such a model could predict the degradation rate of plastics, representing a substantial advancement in biodegradable polymer research.

Environmental implication

This paper clearly shows that all the physico-chemical parameters studied in the literature actually converge on a single parameter: the glass transition temperature of soaked material (T_g^s). By incorporating the effect of T_g^s into a predictive kinetic model, this research could provides will offers a faster and more reliable way to evaluate the degradation rates of plastics well before they are marketed.

This innovation is a significant step forward in the development of biodegradable plastics, as it can substantially reduce the time and resources required to assess plastic waste management.

CRediT authorship contribution statement

Delacuvellerie Alice: Writing – review & editing, Methodology,

Funding acquisition, Supervision, Conceptualization. **Benali Samira:** Writing – review & editing, Methodology, Funding acquisition, Supervision, Conceptualization. **Dufour Sylvie Colette:** Writing – review & editing, Writing – original draft, Methodology, Formal analysis, Conceptualization, Funding acquisition, Investigation. **Raquez Jean-Marie:** Writing – review & editing, Supervision, Methodology, Conceptualization, Funding acquisition, Project administration, Resources. **Wattiez Ruddy:** Supervision, Conceptualization, Funding acquisition, Project administration, Resources, Methodology, Writing – review & editing. **Dubois Philippe:** Writing – review & editing. **Paint Yoann:** Investigation, Writing – review & editing.

Declaration of Competing Interest

The authors declare that they have no known competing financial interests or personal relationships that could have appeared to influence the work reported in this paper.

Acknowledgments

This work was supported by the Fonds de la Recherche Scientifique - FNRS: Sylvie Dufour is a FRIA grantee.

Appendix A. Supporting information

Supplementary data associated with this article can be found in the online version at doi:10.1016/j.jhazmat.2025.138544.

Data Availability

No data was used for the research described in the article.

References

[1.] Faits et Chiffres Sur Le Monde Des Polymères Synthétiques. Atlas Du Plast, 2020.
[2.] Issac, M.N., Kandasubramanian, B., 2021. Effect of microplastics in water and aquatic systems. Environ Sci Pollut Res 28, 19544–19562.
[3] Sunagawa, S., Acinas, S.G., Bork, P., Bowler, C., Tara Oceans Coordinators, S.G., Acinas, M., Babin, P., Bork, E., Boss, C., Bowler, G., Cochrane, C., De Vargas, M., Follows, G., Gorsky, N., Grimsley, L., Guidi, P., Hingamp, D., Iudicone, O., Jaillon, S., Kandels, L., Karp-Boss, E., Karsenti, M., Lescot, F., Not, H., Ogata, S., Pesant, N., Poulton, J., Raes, C., Sardet, M., Sieracki, S., Speich, L., Stemmann, M. B., Sullivan, S., Sunagawa, P., Wincker, D., Eveillard, G., Gorsky, L., Guidi, D., Iudicone, E., Karsenti, F., Lombard, H., Ogata, S., Pesant, M.B., Sullivan, P., Wincker, C., De Vargas, 2020. Tara Oceans: towards global ocean ecosystems biology. Nat Rev Microbiol 18, 428–445.
[4.] Barnes, D.K.A., Galgani, F., Thompson, R.C., Barlaz, M., 2009. Accumulation and fragmentation of plastic debris in global environments. Philosophical transactions of the royal society. B: Biol Sci 364, 1985–1998.
[5.] Rosenboom, J.-G., Langer, R., Traverso, G., 2022. Bioplastics for a circular economy. Nat Rev Mater 7, 117–137.
[6] P. Skoczinski, M. Carus, G. Tweddle, P. Ruiz, D. de Guzman, J. Ravenstijn, H. Käb, N. Hark, L. Dammer, "Bio-based Building Blocks and Polymers – Global Capacities, Production and Trends 2022-2027" (nova-Institut GmbH, 2023).
[7.] Zeb, A., Liu, W., Ali, N., Shi, R., Wang, Q., Wang, J., Li, J., Yin, C., Liu, J., Yu, M., Liu, J., 2024. Microplastic pollution in terrestrial ecosystems: global implications and sustainable solutions. J Hazard Mater 461, 132636.
[8.] Andrady, A.L., 2011. Microplastics in the marine environment. Mar Pollut Bull 62, 1596–1605.
[9.] Cottom, J.W., Cook, E., Velis, C.A., 2024. A local-to-global emissions inventory of macroplastic pollution. Nature 633, 101–108.
[10.] Ellis, L.D., Rorrer, N.A., Sullivan, K.P., Otto, M., McGeehan, J.E., Román-Leshkov, Y., Wierckx, N., Beckham, G.T., 2021. Chemical and biological catalysis for plastics recycling and upcycling. Nat Catal 4, 539–556.
[11.] Dubois, P., 2022. Reactive Extrusion (REx): using chemistry and engineering to solve the problem of ocean plastics. Engineering 14, 15–18.
[12.] Lamberti, F.M., Román-Ramírez, L.A., Wood, J., 2020. Recycling of bioplastics: routes and benefits. J Polym Environ 28, 2551–2571.
[13.] Tournier, V., Topham, C.M., Gilles, A., David, B., Folgoas, C., Moya-Leclair, E., Kamionka, E., Desrousseaux, M.-L., Texier, H., Gavalda, S., Cot, M., Guémard, E., Dalibey, M., Nomme, J., Cioci, G., Barbe, S., Chateau, M., André, I., Duquesne, S., Marty, A., 2020. An engineered PET depolymerase to break down and recycle plastic bottles. Nature 580, 216–219.
[14.] Pu, Shengyan, Liu, Shibin, 2023. Extracell Enzym Environ.
[15.] Bher, A., Mayekar, P.C., Auras, R.A., Schvezov, C.E., 2022. Biodegradation of biodegradable polymers in mesophilic aerobic environments. IJMS 23, 12165.
[16.] Lim, B.K.H., Thian, E.S., 2022. Biodegradation of polymers in managing plastic waste — a review. Sci Total Environ 813, 151880.
[17.] Guicherd, M., Ben Khaled, M., Guéroult, M., Nomme, J., Dalibey, M., Grimaud, F., Alvarez, P., Kamionka, E., Gavalda, S., Noël, M., Vuillemin, M., Amillastre, E., Labourdette, D., Cioci, G., Tournier, V., Kitpreechavanich, V., Dubois, P., André, I., Duquesne, S., Marty, A., 2024. An engineered enzyme embedded into PLA to make self-biodegradable plastic. Nature 631, 884–890.
[18.] Rosli, N.A., Karamanlioglu, M., Kargarzadeh, H., Ahmad, I., 2021. Comprehensive exploration of natural degradation of poly(lactic acid) blends in various degradation media: a review. Int J Biol Macromol 187, 732–741.
[19.] De Jong, S.J., Arias, E.R., Rijkers, D.T.S., Van Nostrum, C.F., Kettenes-van Den Bosch, J.J., Hennink, W.E., 2001. New insights into the hydrolytic degradation of poly(lactic acid): participation of the alcohol terminus. Polymer 42, 2795–2802.
[20] TSUJI, 2010. Hydrolytic Degrad 345–381.
[21.] S. Li, M. Vert, Bioddegradation of aliphatic polyesters. G. Scott (*ed.), Degradable Polymlers, 2nd Edition*, 71–131 (2002).
[22.] Zhang, S., Li, M., Zuo, Z., Niu, Z., 2023. Recent advances in plastic recycling and upgrading under mild conditions. Green Chem 25, 6949–6970.
[23.] Shi, Y., Diao, X., Ji, N., Ding, H., Ya, Z., Xu, D., Wei, R., Cao, K., Zhang, S., 2025. Advances and challenges for catalytic recycling and upgrading of real-world mixed plastic waste. ACS Catal 15, 841–868.
[24.] Fukuzaki, H., Yoshida, M., Asano, M., Kumakura, M., 1989. Synthesis of copoly(d, l-lactic acid) with relatively low molecular weight and in vitro degradation. Eur Polym J 25, 1019–1026.
[25.] Iwata, T., Doi, Y., 1998. Morphology and enzymatic degradation of poly(l -lactic acid) single crystals. Macromolecules 31, 2461–2467.
[26.] Lee, W.-K., Iwata, T., 2008. Morphological study on thermal treatment and degradation behaviors of solution-grown poly(l-lactide) single crystals. Ultramicroscopy 108, 1054–1057.
[27.] Tsuji, H., Ikarashi, K., 2004. In vitro hydrolysis of poly(l-lactide) crystalline residues as extended-chain crystallites. Part I: long-term hydrolysis in phosphate-buffered solution at 37°C. Biomaterials 25, 5449–5455.
[28.] Kawai, F., Nakadai, K., Nishioka, E., Nakajima, H., Ohara, H., Masaki, K., Iefuji, H., 2011. Different enantioselectivity of two types of poly(lactic acid) depolymerases toward poly(l-lactic acid) and poly(d-lactic acid). Polym Degrad Stab 96, 1342–1348.
[29.] Reeve, M.S., McCarthy, S.P., Downey, M.J., Gross, R.A., 1994. Polylactide stereochemistry: effect on enzymic degradability. Macromolecules 27, 825–831.
[30.] Yamashita, K., Kikkawa, Y., Kurokawa, K., Doi, Y., 2005. Enzymatic degradation of poly(l-lactide) film by proteinase k: quartz crystal microbalance and atomic force microscopy study. Biomacromolecules 6, 850–857.
[31.] Tsuji, H., Ishida, T., 2003. Surface hydrophilicities and enzymatic hydrolyzability of biodegradable polyesters, 2. Macromol Biosci 3, 51–58.
[32.] Li, X., Zhang, H., Li, H., Yuan, X., 2010. Encapsulation of proteinase K in PELA ultrafine fibers by emulsion electrospinning: preparation and in vitro evaluation. Colloid Polym Sci 288, 1113–1119.
[33.] R. Auras, L.-T. Lim, S. Selke, H. Tsuji, "Poly(lactic acid): Syntheseis, Structures, Properties, Processing, Applications, and End of Life" (Richard F. Grossman and Domasius Nwabunma, ed. 2nd, 2022), p. 481.
[34.] Chevalier, A., Richard, A., 1827. *Dictionnaire Des Drogues Simples et Composées.* Béchet.,, 2. Béchet.,.
[35.] Panariello, L., Coltelli, M.-B., Buchignani, M., Lazzeri, A., 2019. Chitosan and nano-structured chitin for biobased anti-microbial treatments onto cellulose based materials. Eur Polym J 113, 328–339.
[36] Herrera, N., Roch, H., Salaberria, A.M., Pino-Orellana, M.A., Labidi, J., Fernandes, S.C.M., Radic, D., Leiva, A., Oksman, K., 2016. Functionalized blown films of plasticized polylactic acid/chitin nanocomposite: preparation and characterization. Mater Des 92, 846–852.
[37.] Salaberria, A., H. Diaz, R., Andrés, M., Fernandes, S., Labidi, J., 2017. The antifungal activity of functionalized chitin nanocrystals in poly (lactid acid) films. Materials 10, 546.
[38.] Joseph, B., Sam, R.M., Balakrishnan, P., J. Maria, H., Gopi, S., Volova, T., C. M. Fernandes, S., Thomas, S., 2020. Extraction of nanochitin from marine resources and fabrication of polymer nanocomposites: Recent advances. Polymers 12.
[39.] Beier, S., Bertilsson, S., 2013. Bact chitin Degrad — Mech Ecophysiol Strateg 4, 1–12.
[40.] Svitil, A.L., Ni Chadhain, S.M., Moore, J.A., Kirchman, D.L., 1997. Chitin Degrad Proteins Prod Mar Bact Vibrio harveyi Grow Differ Forms Chitin 63, 408–413.
[41.] Cottrell, M.T., Moore, J.A., Kirchman, D.L., 1999. Chitinases Uncultured Mar Microorg 65, 2553–2557.
[42.] Qi, X., Ren, Y., Wang, X., 2017. New advances in the biodegradation of Poly (lactic) acid. Int Biodeterior Biodegrad 117, 215–223.
[43.] Ilyas, R.A., Sapuan, S.M., Harussani, M.M., Hakimi, M.Y.A.Y., Haziq, M.Z.M., Atikah, M.S.N., Asyraf, M.R.M., Ishak, M.R., Razman, M.R., Nurazzi, N.M., Norrrahim, M.N.F., Abral, H., Asrofi, M., 2021. Polylactic Acid (PLA) biocomposite: processing, additive manufacturing and advanced. Appl Polym 13, 1326.
[44.] Sharma, S., Majumdar, A., Butola, B.S., 2021. Tailoring the biodegradability of polylactic acid (PLA) based films and ramie- PLA green composites by using selective additives. Int J Biol Macromol 181, 1092–1103.
[45.] Jarerat, A., Tokiwa, Y., Tanaka, H., 2004. Microbial poly(l-lactide)-degrading enzyme induced by amino acids, peptides, and poly(l-amino acids). J Polym Environ 12, 139–146.
[46.] Rizvi, R., Cochrane, B., Naguib, H., Lee, P.C., 2011. Fabrication and characterization of melt-blended polylactide-chitin composites and their foams. J Cell Plast 47, 283–300.

[47.] Herrera, N., Salaberria, A.M., Mathew, A.P., Oksman, K., 2016. Plasticized polylactic acid nanocomposite films with cellulose and chitin nanocrystals prepared using extrusion and compression molding with two cooling rates: Effects on mechanical, thermal and optical properties. Compos Part A: Appl Sci Manuf 83, 89–97.
[48.] Singh, A.A., Wei, J., Herrera, N., Geng, S., Oksman, K., 2018. Synergistic effect of chitin nanocrystals and orientations induced by solid-state drawing on PLA-based nanocomposite tapes. Compos Sci Technol 162, 140–145.
[49.] Magnani, C., Fazilati, M., Kádár, R., Idström, A., Evenäs, L., Raquez, J.M., Lo Re, G., 2022. Green topochemical esterification effects on the supramolecular structure of chitin nanocrystals: implications for highly stable pickering emulsions. ACS Appl Nano Mater 5, 4731–4743.
[50.] Pillet, M., 2011. Les plans D'Expériences Par la Méthode TAGUCHI.
[51.] Hsieh, Y.-T., Nozaki, S., Kido, M., Kamitani, K., Kojio, K., Takahara, A., 2020. Crystal polymorphism of polylactide and its composites by X-ray diffraction study. Polym J 52, 755–763.
[52.] Fukushima, K., Tabuani, D., Dottori, M., Armentano, I., Kenny, J.M., Camino, G., 2011. Effect of temperature and nanoparticle type on hydrolytic degradation of poly (lactic acid) nanocomposites. Polym Degrad Stab 96, 2120–2129.
[53.] Hakkarainen, M., 2002. Aliphatic polyesters: abiotic and biotic degradation and degradation products. Adv Polym Sci 157, 113–138.
[54.] Li, S., McCarthy, S., 1999. Further investigations on the hydrolytic degradation of poly (DL-lactide). Biomaterials 20, 35–44.
[55] Tsuji, H., Shimizu, K., Sato, Y., 2012. Hydrolytic Degrad Poly (L -Lact Acid): Comb Eff UV Treat Cryst. https://doi.org/10.1002/app.
[56.] Fischer, E.W., Sterzel, H.J., Wegner, G., 1973. Investigation of the structure of solution grown crystals of lactide copolymers by means of chemical reactions. Kolloid-Z Z FüR Polym 251, 980–990.
[57.] Tsuji, H., Miyauchi, S., 2001. Poly(l-lactide): VI E€ects of crystallinity on enzymatic hydrolysis of poly(l-lactide) without free amorphous region. Polym Degrad Stab.
[58.] Tsuji, H., Mizuno, A., Ikada, Y., 2000. Properties and morphology of poly(L-lactide). III. Effects of initial crystallinity on long-termin vitro hydrolysis of high molecular weight poly(L-lactide) film in phosphate-buffered solution. J Appl Polym Sci 77, 1452–1464.
[59.] Kurokawa, K., Yamashita, K., Doi, Y., Abe, H., 2008. Structural effects of terminal groups on nonenzymatic and enzymatic degradations of end-capped poly(L -lactide). Biomacromolecules 9, 1071–1078.
[60.] H. Tsuji, S. Miyauchi, Poly(l-lactide): 7. Enzymatic hydrolysis of free and restricted amorphous regions in poly(l-lactide) ®lms with different crystallinities and a ®xed crystalline thickness. (2001).
[61.] Aouay, M., Magnin, A., Putaux, J.-L., Boufi, S., 2022. Biobased nucleation agents for poly-L-(lactic acid) — effect on crystallization, rheological and mechanical properties. Int J Biol Macromol 218, 588–600.
[62.] Schmitt, E.A., Flanagan, D.R., Linhardt, R.J., 1994. Importance of distinct water environments in the hydrolysis of poly(DL-lactide-co-glycolide). ACS Publ. https://doi.org/10.1021/ma00081a019.
[63.] Passerini, N., Craig, D.Q.M., 2001. An investigation into the effects of residual water on the glass transition temperature of polylactide microspheres using modulated temperature DSC. J Control Release 73, 111–115.
[64.] Pirzadeh, E., Zadhoush, A., Haghighat, M., 2007. Hydrolytic and thermal degradation of PET fibers and PET granule: The effects of crystallization, temperature, and humidity. J Appl Polym Sci 106, 1544–1549.
[65.] Lima, G.M.R., Mukherjee, A., Picchioni, F., Bose, R.K., 2022. Biodegradable PBAT, PBS and PHBV polymers characterization for porous structure: further steps to sustainable plastics. Preprint. https://doi.org/10.21203/rs.3.rs-2154343/v1.
[66.] Tsuji, H., Ikada, Y., 1997. Blends of crystalline and amorphous poly(lactide). III. Hydrolysis of solution-cast blend films. J Appl Polym Sci 63, 855–863.
[67.] Hyon, S.H., Jamshidi, K., Ikada, Y., 1997. Synthesis of polylactides with different molecular weights. Biomaterials 18, 1503–1508.
[68.] Hyon, S.-H., Jamishidi, K., Ikada, 1998. Effects of residual monomer on the degradation of DL-lactide polymer. Polym Int 46, 196–202.
[69.] Pan, P., Zhu, B., Kai, W., Dong, T., Inoue, Y., 2008. Effect of crystallization temperature on crystal modifications and crystallization kinetics of poly(L-lactide). J Appl Polym Sci 107, 54–62.
[70.] Zhang, Nan, Yu, Xu, Duan, Jin, Yang, Jing-hui, Huang, Ting, Qi, Xiao-dong, Wang, Yong, 2018. Comparison study of hydrolytic degradation behaviors between α′- and α-poly(Llactide). Polym Degrad Stab 148.